Coupled Traffic–Power Optimization for Integrated Energy Service Stations under Electric Heavy-Duty Truck Demand

Senyao Wang, Jin Ma, and Thomas Chaffey
School of Electrical and Computer Engineering, The University of Sydney, Sydney, Australia
Email: senyao.wang@sydney.edu.au, j.ma@sydney.edu.au, thomas.chaffey@sydney.edu.au

***Abstract*—Integrated Energy Service Stations (IESSs) have become the mainstream solution for electric heavy-duty truck (EHDT) operations, enabling rapid battery swapping and large-scale fleet electrification. However, the rising high-power swapping demand poses new challenges to distribution network security and coordinated logistics planning. To address these issues, this paper proposes a coupled traffic–power optimization framework that embeds distribution-network constraints and dynamic electricity prices into a vehicle routing problem with time windows (VRPTW). The model jointly optimizes routing, battery swapping, and grid interaction to balance logistics efficiency and grid reliability. Case studies on a 100-node road network coupled with an IEEE 118-bus distribution system show that the proposed method reduces total operating cost by 24.8%, increases task fulfillment by 12.3%, and shortens total service time by 8.6% compared with the benchmark, while the time-cost component decreases by 18.6%. These results show that integrated traffic–power scheduling improves fleet efficiency and grid stability.**

***Index Terms*—Integrated Energy Service Station (IESS), Electric heavy-duty truck (EHDT), VRPTW, Battery swapping scheduling, Distribution network security**

NOMENCLATURE

Abbreviations:

EHDT	Electric Heavy-Duty Truck
IESS	Integrated Energy Service Station
VRPTW	Vehicle Routing Problem with Time Windows

Sets:

K	Set of vehicles
C	Set of customers
S	Set of swapping stations
D	Set of depots
L	Set of nodes, $L = C \cup S \cup D$
$\mathbf{V}$	Set of virtual routes/trips (index v)
$\mathbf{T}$	Set of time slots
$\mathcal{B}$	Set of distribution-network buses
t	Time index

Decision variables:

$x_{v,i,j,k,t}$	Vehicle k uses arc $i \to j$ (trip v) at t.
$y_{n,k,t}$	Vehicle k serves node n at t.
$s_{s,k,t}$	Vehicle k swaps at station s at t.
$SOC_{n,k,t}$	SOC of vehicle k at node n and time t.
$SOC_{i,k,t}^{dep}$	Departure SOC from node i at t.
$W_{n,k,t}$	Load of vehicle k at node n and time t.

Parameters:

d_{ij}	Distance between nodes i and j.
t_{ij}	Travel time between nodes i and j.
Q_k	Battery capacity of vehicle k.
ν_0	Base energy consumption rate.
ν_w	Weight-dependent energy coefficient.
M	Big-M constant.
$c_{b,t}, c_{s,t}$	Electricity buying/selling price at time t.
$P_{ij,t}$	Active power flow on line (i, j).
$Q_{ij,t}$	Reactive power flow on line (i, j).
$S_{ij}^{\max}$	Thermal capacity of line (i, j).
$V_{i,t}$	Voltage magnitude at bus i.
$V^{\min}/V^{\max}$	Voltage lower and upper bounds.

I. INTRODUCTION

Transportation electrification is expanding from port and mining operations to urban and inter-city heavy-duty logistics. As EHDT fleets grow, charging and swapping facilities are being rapidly deployed along transport corridors and logistics hubs. This expansion raises two challenges: on the transport side, fast charging causes high time and economic costs due to long dwell and queuing; on the power side, large-scale high-power connections strain distribution-network security (voltage, thermal, and transformer limits). To address these issues, Integrated Energy Service Stations (IESSs) have emerged as grid-interactive swapping hubs that integrate local renewables, provide faster service through on-site battery inventory, and act as flexible grid resources for peak shaving and ancillary services.

Recent research has increasingly focused on integrating routing, task scheduling, and energy decisions into unified models for HDT fleets. [1] proposed a scalable joint routing–charging (JRC) scheduling framework using surrogate Lagrangian relaxation. [2] and [3] addressed heterogeneous charging technologies and uncertain energy consumption via branch–price–and–cut and robust optimization, respectively. Distributed and data-driven coordination models were studied in [4], [5], [6], highlighting scalability in large and dynamic fleet systems. Further, [7] incorporated platooning and driver assignment into highway network routing, while [8], [9] explored solar pavement-enabled power networks and quantum-enhanced scheduling methods. [10] and [11] extended the

979-8-3315-8138-1

problem to consider driver behavioral differences and life-cycle emissions, enriching the scope of multi-objective fleet optimization.

Parallel efforts have advanced the planning, operation, and grid integration of high-capacity battery swapping hubs. [12], [13] developed integrated models to compare fast charging and battery swapping and to jointly optimize siting, sizing, and operation of highway swapping stations. Real-time scheduling and flexibility for grid support were addressed in [14], [15], emphasizing microgrid coupling and hybrid control. [16] further explored photovoltaic-enabled highways and the role of mobile energy storage in charging–swapping coordination. Additionally, [17], [18] proposed bi-objective and metaheuristic strategies to enhance routing and assignment under shared infrastructure constraints. The integration of multi-task, multi-trip vehicle scheduling in industrial settings was also explored by [19], demonstrating the relevance of these models beyond conventional logistics.

However, three gaps remain for inter-city EHDT operations with IESSs. (1) The task-driven nature of EHDT routing and cargo scheduling (pickup/delivery quantities and time windows) remains unintegrated with station queuing and spare-pack turnover, so the endogenous impact on fleet cost and time efficiency is not captured within a unified loop. (2) Under large-scale IESS interconnections, the coupling between distribution-network security limits (voltage, thermal, and transformer constraints) and station power–time decisions is rarely modeled; distribution-level OPF seldom provides time-varying feasible envelopes and marginal prices for secure, value-revealing scheduling. (3) The coordinated use of local renewables and inventory batteries as flexible grid resources is largely absent; a unified framework is needed to leverage them for peak shaving, congestion relief, and frequency regulation under uncertainty.

Figure 1 illustrates the overall technical roadmap of the proposed work, highlighting the interaction between traffic and distribution layers within the IESS framework. The rest of this paper is organized as follows. Section II presents the modeling framework, Section III describes the optimization method, Section IV provides case studies, and Section V concludes the paper.

II. Coupled Traffic–Power System Framework

We consider a task-driven EHDT operation that starts from a depot, serves customer tasks within time windows, and returns to the depot. Vehicle routing and task timing on the transportation side determine time-varying swapping demands at IESSs. Each IESS is connected to a distribution-network bus and behaves as a high-power, bidirectional, grid-interactive node. Routing and task scheduling induce time–space swapping power at IESS buses, while network security constraints and marginal price signals feed back to routing and swapping decisions.

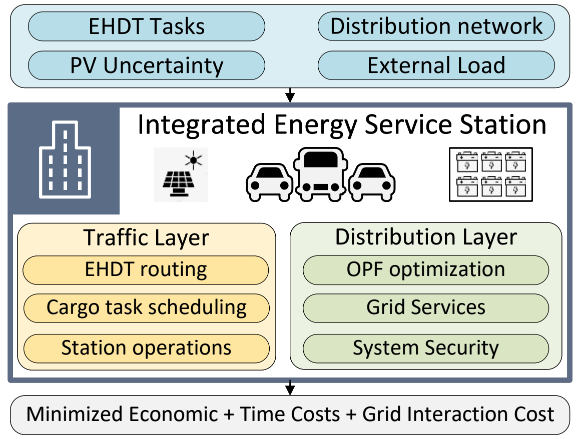

Fig. 1. Technical roadmap of the coupled traffic–power framework.

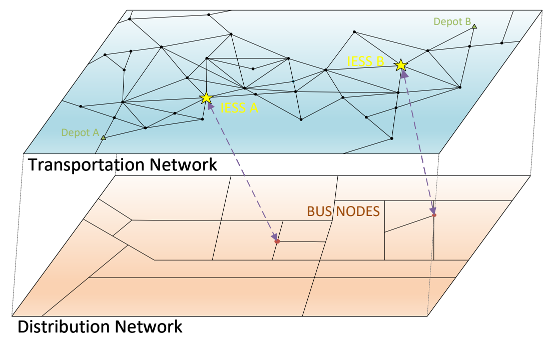

Fig. 2. Dual-network schematic. Routing determines swapping demand at IESS nodes; the grid provides feasible limits and price signals.

A. Objective function

The unified multi-objective optimization problem is defined as

$$\min Z = \sum_{t \in T} \left(w_L C_{L,t} + w_E C_{E,t} + w_G C_{G,t} \right), \tag{1}$$

where w_L, w_E, and w_G are the relative weights of logistics, energy service, and grid interaction costs, respectively, with $w_L + w_E + w_G = 1$.

B. Cost decomposition

1) Logistics cost $C_{L,t}$:

$$\begin{aligned} C_{L,t} = & \sum_{v \in V} \sum_{i,j \in L} \sum_{k \in K} c_d \, d_{ij} \, x_{v,i,j,k,t} \\ & + c_w \, \Delta t + \sum_{v \in V} \sum_{n \in C} \sum_{k \in K} c_p \, \max\left(0, \, a_{v,n,k} - T_n\right), \end{aligned} \tag{2}$$

where c_d is the unit travel cost, d_{ij} is the distance between nodes i and j, $x_{v,i,j,k,t}$ is the routing decision, c_w is the driver wage rate, Δt is the service interval, c_p is the tardiness penalty coefficient, $a_{v,n,k}$ is the service time of vehicle v at node n, and T_n is the deadline.

979-8-3315-8138-1

2) Energy service cost $C_{E,t}$:

$$C_{E,t} = \sum_{s\in S} c_{b,t}\, P^{+}_{s,t} - \sum_{s\in S} c_{s,t}\, P^{-}_{s,t} + \sum_{s\in S}\sum_{k\in K} C_{\text{deg},skt}, \tag{3}$$

where $c_{b,t}$ and $c_{s,t}$ are electricity purchase and selling prices at time t, $P^{+}_{s,t}$ is grid power purchased, $P^{-}_{s,t}$ is grid power injected, and $C_{\text{deg},skt}$ is the degradation cost for a swap of vehicle k at station s in slot t.

3) Grid interaction cost $C_{G,t}$:

$$C_{G,t} = c_d^{*}\, \max\Big(\sum_{s\in S} P^{+}_{s,t}, 0\Big) + c_v \sum_{j\in\mathcal{B}} \Big[\max(0, V^{\min} - V_{j,t}) + \max(0, V_{j,t} - V^{\max})\Big]. \tag{4}$$

where c_d^{*} is the demand charge coefficient, $\sum_s P^{+}_{s,t}$ is the net power imported, c_v is the voltage penalty coefficient, $V_{j,t}$ is the bus voltage magnitude, and $[V_{\min}, V_{\max}]$ are the lower and upper voltage limits.

The objective in (1) combines (2)–(4) into a unified criterion. The feasible region includes (i) traffic-layer routing/task/SOC dynamics and (ii) IESS–grid energy balance and security constraints (Section III).

III. Integrated VRPTW–IESS Formulation

Building on the coupled traffic–power system framework in Section II, this section develops the integrated formulation of VRPTW and IESS operation. The model captures both the task-driven logistics constraints and the grid-aware station constraints, providing the feasible region for the multi-objective optimization.

A. VRPTW-based logistics formulation

Vehicles start from depots, serve customer tasks within time windows, and return to depots. The following constraints govern initial conditions, state propagation, node operations, and return.

1) Initial conditions:

$$\begin{aligned} A_{dk} &= D_{dk} = 0, && (d\in D,\ k\in K),\\ SOC_{dk} &= SOC^{0}_{k}, && (d\in D,\ k\in K),\\ W_{dk} &= W^{0}, && (d\in D,\ k\in K), \end{aligned} \tag{5}$$

where A_{dk}, D_{dk} are arrival and departure times at depot d, SOC^{0}_{k} the initial SOC of vehicle k, and W^{0} the empty weight.

2) State propagation:

$$e_{v,i,j,k,t} = (\nu_0 + \nu_w W_{i,k,t})\, d_{ij}, \tag{6}$$

$$\begin{aligned} A_{j,k,t} &\ge D_{i,k,t} + t_{ij} - M\,(1 - x_{v,i,j,k,t}),\\ SOC_{j,k,t} &\le SOC^{dep}_{i,k,t} - e_{v,i,j,k,t} + M\,(1 - x_{v,i,j,k,t}),\\ SOC_{j,k,t} &\ge SOC^{dep}_{i,k,t} - e_{v,i,j,k,t} - M\,(1 - x_{v,i,j,k,t}),\\ W_{j,k,t} &\le W_{i,k,t} - w_j\, y_{n,k,t} + M\,(1 - x_{v,i,j,k,t}),\\ W_{j,k,t} &\ge W_{i,k,t} - w_j\, y_{n,k,t} - M\,(1 - x_{v,i,j,k,t}), \end{aligned} \tag{7}$$

where $e_{v,i,j,k,t}$ is the load-dependent energy consumption of virtual trip v for vehicle k moving from i to j at time t, t_{ij} is the travel time, and M is a sufficiently large constant.

$$\sum_{v\in V}\sum_{i\in L}\sum_{j\in L} x_{v,i,j,k,t} \le 1, \quad \forall k\in K,\ t\in T, \tag{8}$$

which ensures that each vehicle k can traverse at most one arc in any time slot t.

3) Node operations and time windows:

$$\begin{aligned} & D_{n,k,t} \ge A_{n,k,t} + T^{svc}_{n} - M\,(1 - y_{n,k,t}),\\ & D_{s,k,t} \ge A_{s,k,t} + T^{swp}_{s}\, s_{s,k,t} - M\,(1 - y_{s,k,t}),\\ & s_{s,k,t} \le y_{s,k,t},\\ & \delta_{n,k,t} \ge A_{n,k,t} - T_n, \quad \delta_{n,k,t} \ge 0,\\ & \eta_{n,k,t} \ge \underline{SOC} - SOC_{n,k,t}, \quad \eta_{n,k,t} \ge 0, \end{aligned} \tag{9}$$

where T^{svc}_{n} is customer service time, T^{swp}_{s} swap duration, $\delta_{n,k,t}$ tardiness slack, and $\eta_{n,k,t}$ SOC slack.

$$\sum_{k\in K}\sum_{v\in V}\sum_{i\in L}\sum_{t\in T} x_{v,i,n,k,t} \le 1, \quad \forall n\in C, \tag{10}$$

$$\sum_{v\in V}\sum_{i\in L}\sum_{t\in T} x_{v,i,n,k,t} = y_{n,k,t}, \quad \forall n\in C,\ k\in K, \tag{11}$$

which ensure that each customer is served at most once and link routing with service decisions.

4) Swapping and return:

$$SOC^{dep}_{i,k,t} = SOC_{i,k,t} + \sum_{s\in S} s_{s,k,t}\,(Q_k - SOC_{i,k,t}), \tag{12}$$

$$p^{\text{swap}}_{s,t} = \frac{E_{\text{pack}}}{\Delta t} \sum_{k\in K} s_{s,k,t}, \quad \forall s\in S, t\in T, \tag{13}$$

$$\begin{aligned} \tau_k &\ge D_{i,k,t} + t_{id} - M\,(1 - x_{v,i,d,k,t}),\\ & \forall d\in D,\ i\in L,\ k\in K,\ t\in T, \end{aligned} \tag{14}$$

where $SOC^{dep}_{i,k,t}$ is departure SOC, $s_{s,k,t}$ is the swapping decision at station s, Q_k is the battery capacity, E_{pack} is the pack energy, and τ_k is the return time of vehicle k.

B. IESS and power-system formulation

Each IESS is mapped to a distribution-network bus, where its demand from VRPTW operations interacts with local BESS, PV generation, and grid constraints. The following equations specify station energy balance and network security.

1) Station energy balance and BESS dynamics:

$$p_{g,st} + p^{pv}_{st} + p^{dis}_{st} = p^{\text{swap}}_{s,t} + p^{EV}_{st} + p^{ch}_{st} + p^{aux}_{st}, \tag{15}$$

$$E_{s,t} = E_{s,t-1} + \Big(\eta^{ch}\, p^{ch}_{s,t} - \frac{1}{\eta^{dis}}\, p^{dis}_{s,t}\Big)\,\Delta t, \tag{16}$$

where $p_{g,st}$ is grid purchase, p^{pv}_{st} PV generation, $p^{ch}_{st}, p^{dis}_{st}$ BESS charge/discharge power, $E_{s,t}$ BESS energy, p^{EV}_{st} other EV demand, and p^{aux}_{st} auxiliary load.

979-8-3315-8138-1

TABLE I
MAIN SIMULATION PARAMETERS

Param.	Setting	Param.	Setting
Depots	2	Truck battery pack	282 kWh
Swap stations	10	Spare packs / station	8 packs
Customers	50	Swap duration	15 min
Trucks	10 EHDTs		

2) Bus mapping and nodal power balance:

$$P_{b,t}^{load} = P_{b,t}^{base} + \sum_{s:\, m(s)=b} p_{g,st}, \tag{17}$$

$$P_{i,t}^{gen} - P_{i,t}^{load} + \sum_{k\in\Omega_i} P_{ik,t} = 0, \tag{18}$$

where $m(s) = b$ maps station s to bus b, $P_{b,t}^{base}$ is base load, $P_{i,t}^{gen}$ generation at bus i, $P_{i,t}^{load}$ total load, and Ω_i the neighbor set of bus i.

3) Voltage and thermal constraints:

$$V_{j,t} = V_{i,t} - 2(r_{ij}P_{ij,t} + x_{ij}Q_{ij,t}), \tag{19}$$

$$V^{\min} \le V_{i,t} \le V^{\max}, \quad P_{ij,t}^2 + Q_{ij,t}^2 \le (S_{ij}^{\max})^2, \tag{20}$$

where (r_{ij}, x_{ij}) are line parameters, $V_{i,t}$ bus voltage, and $S_{ij}^{\max}$ line rating.

By combining these VRPTW and IESS–grid constraints, the integrated formulation bridges logistics operations and power-system security, ensuring feasibility of the unified optimization problem.

IV. CASE STUDY

The case study is conducted on the coupled test system summarized in Table I, consisting of a 100-node road network connected to the IEEE 118-bus distribution system. Each IESS is mapped to a distribution-network bus. Off-vehicle spare battery packs serve as controllable energy buffers for swapping operations. Electricity prices and baseline loads are treated as exogenous inputs to the optimization layer. All simulations are implemented in Python 3.10 and solved using GUROBI, with a termination criterion of global optimality or a 10^{-3} MIP gap.

A. Logistics Optimization Analysis

Figure 3 shows the optimized routing of the EHDT fleet on the transportation network. The coupled traffic–power optimization achieves 8.6% shorter total service time and 12.3% higher task fulfillment than the benchmark. Concretely, the duration-based total service time decreases by 8.6%, whereas the time-cost component (Table II) decreases by 18.6%. Routes are hub-oriented around high-centrality IESS nodes, enabling swaps with minimal detours and forming stable, low-overlap corridors. These results demonstrate improved delivery efficiency and coordinated fleet organization.

Figure 4 depicts a representative vehicle's SOC, payload, and unit-energy profile. The SOC remains stable within bounds, and the vehicle completes its loop on schedule, confirming that the integrated model effectively synchronizes routing and energy management.

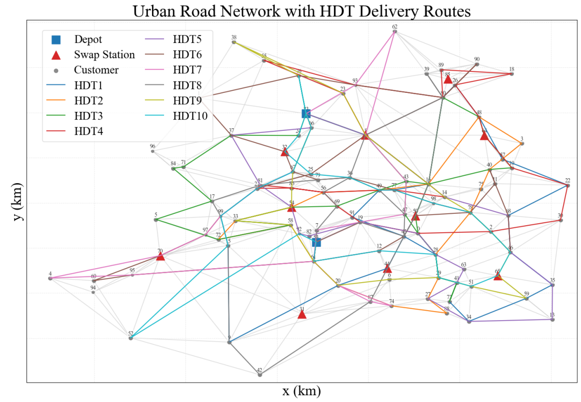

Fig. 3. Optimized vehicle routing solution on the test road network. The figure shows depots, customer nodes, swapping stations, and the computed routes of each vehicle. Vehicles depart from depots, serve assigned customers, utilize IESS nodes for battery swapping when required, and return to their depots.

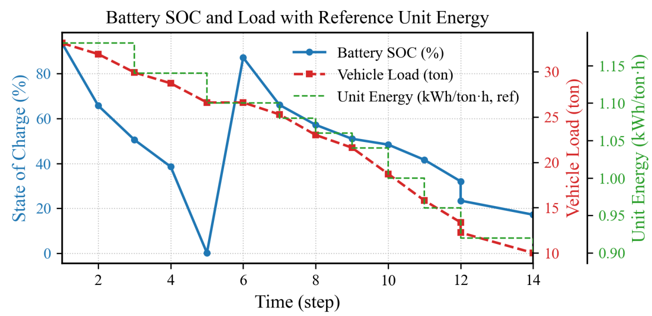

Fig. 4. Representative EHDT delivery cycle showing SOC, payload, and unit energy evolution.

B. Economic Operation Analysis

Table II presents the cost breakdown of the proposed and benchmark models. The total operating cost decreases from $8.27{\times}10^3$ to $6.22{\times}10^3$ (–24.8%), driven by more compact routing and reduced waiting at IESS nodes. Swap cost falls from $1.51{\times}10^3$ to $0.72{\times}10^3$, and grid purchases drop from $1.94{\times}10^3$ to $0.85{\times}10^3$, showing effective alignment with low-price periods. Despite a slight decline in grid selling revenue, overall expenditure remains lower. These results indicate that traffic–power co-optimization alleviates temporal and spatial inefficiencies in fleet operation. Unlike the benchmark, where four vehicles violated the minimum SOC limit, all vehicles in the proposed model maintained feasible SOC, confirming enhanced energy planning and operational security.

C. Grid Security Analysis

Table III compares the grid-side performance of the base and proposed models. The base case shows a mean voltage offset of 0.0190 p.u. and a maximum deviation of 0.111 p.u., exceeding the secure range (0.95–1.05 p.u.) and resulting in seven voltage violations. These fluctuations stem from uncoordinated charging and frequent swapping that create repeated voltage perturbations. Under the proposed coupled optimiza-

979-8-3315-8138-1

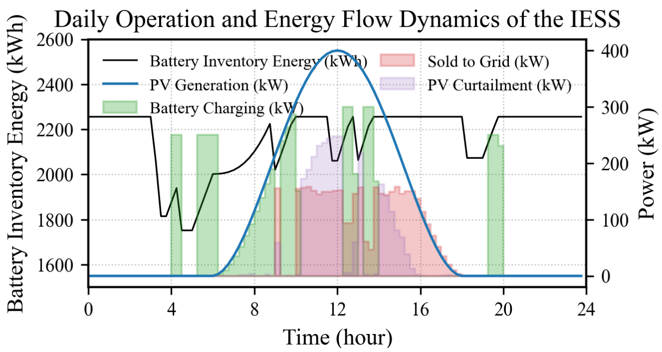

Fig. 5. Daily Operation and Energy Flow Dynamics of the IESSs

TABLE II
COMPARISON OF LOGISTICS AND ENERGY-RELATED COSTS BETWEEN MODELS

Model	**Vehicle base**	**Time cost**	**Swap cost**	**Grid buy**	**Total**
Proposed	1800	4773.85	720.00	847.20	6221.39
Benchmark	1800	5862.45	1505.36	1941.09	8270.69

tion, the mean voltage offset rises slightly to 0.0309 p.u., but the maximum deviation decreases to 0.047 p.u., and no voltage violations occur. The load satisfaction rate improves markedly from 68.99% to 97.33%, indicating smoother nodal voltage profiles and better grid–station coordination.

V. CONCLUSION

We proposed a coupled traffic–power optimization framework for EHDT–IESS operations. By embedding distribution-network constraints and time-varying electricity prices into a VRPTW model, the framework co-optimizes routing, battery swapping, and grid interaction to achieve both logistics efficiency and grid security. On a 100-node road network coupled with the IEEE 118-bus system, the method reduces total operating cost by 24.8%, increases task fulfillment by 12.3%, and eliminates voltage violations. These results indicate that synchronized traffic–power scheduling improves voltage stability, reduces power-exchange fluctuations, and enhances overall grid reliability. Future work will incorporate stochastic traffic demand and price uncertainties via multi-period chance-constrained and distributionally robust formulations, and validate scalability and reproducibility on real road–distribution network data.

TABLE III
GRID PERFORMANCE UNDER BASE AND PROPOSED MODELS

Scenario	**Mean offset**	**Max dev.**	**Load sat. (%)**	**Viol.**
Base Model	0.0190	0.111	68.99	7
This Model	0.0309	0.047	97.33	0

REFERENCES

[1] M. A. Bragin, Z. Ye, and N. Yu, “Toward efficient transportation electrification of heavy-duty trucks: Joint scheduling of truck routing and charging,” *Transportation Research Part C: Emerging Technologies*, vol. 160, p. 104494, 2024.

[2] G. M. Nafstad, G. Desaulniers, and M. Stålhane, “Branch-price-and-cut for the electric vehicle routing problem with heterogeneous recharging technologies and nonlinear recharging functions,” *Transportation Science*, vol. 59, no. 3, pp. 628–646, 2025.

[3] A. Amiri, H. Zolfagharinia, and S. H. Amin, “A robust multi-objective routing problem for heavy-duty electric trucks with uncertain energy consumption,” *Computers & Industrial Engineering*, vol. 178, p. 109108, 2023.

[4] Y. Tao, J. Qiu, S. Lai, X. Sun, H. Liu, and J. Zhao, “Distributed electric vehicle assignment and charging navigation in cyber-physical systems,” *IEEE Transactions on Smart Grid*, vol. 15, no. 2, pp. 1861–1875, 2023.

[5] H. Miao, S. Chen, M. Cao, and Z. Yang, “Efficient algorithm for large scale electric vehicle routing problem with charging capacity constraint,” *IEEE Transactions on Intelligent Transportation Systems*, 2025.

[6] J. K. Yap, V. M. Baskaran, W.-S. Tan, Z. Y. Ding, H. Wang, and D. L. Dowe, “Transformer-based deep learning model for joint routing and scheduling with varying electric vehicle numbers,” in *2025 IEEE Industry Applications Society Annual Meeting (IAS)*. IEEE, 2025, pp. 1–8.

[7] X. Yan, M. Xu, and X. Sun, “Electric truck routing and platooning problem considering vehicle charging and driver assignment on highway networks,” *Transportation Research Part C: Emerging Technologies*, vol. 173, p. 105072, 2025.

[8] B. Shi, W. Dai, H. Liu, and H. H. Goh, “Link-based distributed co-optimization of power dispatch and ev routing in solar pavement-enabled power-transportation networks,” *IEEE Transactions on Sustainable Energy*, 2025.

[9] U. Khalid, U. I. Paracha, S. M. A. Rizvi, and H. Shin, “Quantum computing for intelligent transportation systems: Vqe-based traffic routing and ev charging scheduling,” *Mathematics*, vol. 13, no. 17, p. 2761, 2025.

[10] Q. Feng, D. Bai, R. Feng, and B. Yu, “Coordinated scheduling of mixed bus fleets and drivers on a single route considering driving habit differences,” *Journal of Transportation Engineering, Part A: Systems*, vol. 151, no. 11, p. 04025090, 2025.

[11] D. Bao, J. Chu, Y. Chen, and Y. Yan, “A life cycle assessment of electric towing vehicle routing problem with time windows: Three-stage linear charging and partial charging strategy,” *Journal of Air Transport Management*, vol. 131, p. 102908, 2026.

[12] R. Wang, A. Martinez, Z. Allybokus, W. Zeng, N. Obrecht, and S. Moura, “Electrifying heavy-duty trucks: Battery-swapping vs fast charging,” *IEEE Transactions on Smart Grid*, 2025.

[13] X. Hao, M. Cao, L. Li, S. Zhang, X. Meng, B. Liu, and H. Wang, “A two-layer programming for highway heavy-duty truck battery swapping stations,” *Energy*, vol. 321, p. 135461, 2025.

[14] H. E. O. Farias, C. A. S. Rangel, B. Z. Franciscatto, H. Klein, L. S. Neves, and V. Gomes, “Combined real-time and scheduling methodology for operation of battery swapping stations considering energy flexibility and grid support,” *Applied Energy*, vol. 397, p. 126332, 2025.

[15] M. S. Gull, M. Khalid, and N. Arshad, “Multi-objective optimization of battery swapping station to power up mobile and stationary loads,” *Applied Energy*, vol. 374, p. 124064, 2024.

[16] D. Wang, J. Guo, Y. Zhang, T. Feng, and C. Zhang, “Enhancing solar energy generation utilization along highways: optimizing electric vehicle charging-swapping schemes and scheduling mobile energy storage systems,” *Applied Energy*, vol. 399, p. 126389, 2025.

[17] S. Pan, R. Wei, X. C. Liu, J. Phillips, and B. Wang, “Strategic bi-objective optimization for electric vehicle fleet replacement leveraging shared charging facilities,” *Computers, Environment and Urban Systems*, vol. 122, p. 102353, 2025.

[18] S. Zhou, D. Zhang, S. Fang, and S. Li, “An adaptive hybrid neighborhood search algorithm for the electric vehicle pickup and delivery problem with time windows and partial charging,” *Swarm and Evolutionary Computation*, 2025.

[19] F. Chang, C. T. Ng, F. Chang, F. Wu, T. Cheng, and L. Zheng, “A multi-task-driven multi-trip electric vehicle routing optimisation method for smart factory,” *Journal of Engineering Design*, pp. 1–32, 2025.

979-8-3315-8138-1